

# Fermion pairing with population imbalance: energy landscape and phase separation in a constrained Hilbert subspace

Zheng-Cheng Gu<sup>†,††</sup>, Geoff Warner<sup>†</sup> and Fei Zhou<sup>†</sup>

*Department of Physics and Astronomy, The University of British Columbia, Vancouver, B.C., Canada V6T1Z1<sup>†</sup>*  
*Center for Advanced Study, Tsinghua University, Beijing, China, 100084<sup>††</sup>*

(Dated: January 11, 2022)

In this Letter we map out the mean field energy potential landscape of fermion pairing states with population imbalance near broad Feshbach Resonances. We apply the landscape to investigate the nature of phase separation, when the Hilbert space is subject to the constraint of constant population imbalance. We calculate the scattering length dependence of the critical population imbalance for various phase separated states across Feshbach resonances.

Recently, cold atom pairing states with population differences were studied experimentally by the MIT and the Rice University cold atom groups[1, 2]. Fermion pairing with population imbalance has been a fascinating subject for a long time and was studied in various contexts [3, 4, 5, 6, 7, 8]. For cold atoms, pairing occurs between two hyperfine states participating in Feshbach resonances, as indicated by experiments a few years ago[9]. Cold atom superfluids across Feshbach resonances with population imbalance have also been studied theoretically, to some extent; different phases were proposed, based on a variety of arguments or calculations[10, 11, 12]. Most recently, cold atom superfluids with population imbalance in finite traps were addressed[13]. It is generally believed that such superfluids exhibit different behaviors on either side of resonances. In the BCS limit, where the scattering length is negative and small in magnitude, the superfluid undergoes a first-order phase transition to a LOFF state (pairing between nonzero total momentum), followed by a second order phase transition to a partially polarized normal state, as the difference in chemical potentials between the two spin species is increased[5, 6]. On the other hand, on the far BEC side where the scattering length is positive and small, one has a continuous transition to a superfluid state coexisting with a Fermi sea composed of the excess spin species.

One of the unique features of cold atoms is that relaxation processes including the (global) population imbalance relaxation are very slow compared to the experimental measurement time period. Therefore, for cold atoms the population imbalance  $P_{im}$  can be considered to be *independent* of  $I$ , the energy splitting between two fermions with the same momentum. This is opposed to traditional solid state, many-body systems where the chemical potential difference between the two species is a unique function of  $I$ , the Zeeman splitting energy, in equilibrium. For cold atoms, the relevant ground state is therefore the state of lowest energy in the constrained Hilbert space defined by fixed total particle number  $N$  and population imbalance  $P_{im}$ , not the lowest energy states in the whole Hilbert space for a given total den-

sity. Motivated by the above observation and the recent experiments on cold atom pairing, in this article we map out the energy potential( $\mathcal{EP}$ ) landscape of all lowest energy homogeneous states in different subspaces specified by  $P_{im}$ . (We leave out discussions on LOFF or other more exotic competing translational-symmetry-breaking states in this article.) The landscape not only provides important information on the energetics of various states but is also critically valuable for the understanding of phase separation phenomena (see below). Furthermore, it paves the way for future studies of the dynamics of superfluids in the limit of slow relaxation. As the first application, we study the phase separation with the help of the landscape and construct phase separated states at a given population imbalance  $P_{im}$  (and with a given density  $\rho$ ). Finally we investigate critical population imbalance for various phase separated states across Feshbach resonances.

The phase separation phenomenon discussed here only occurs when we consider states in a Hilbert subspace with a conserved population imbalance. These phase separated states generally do not correspond to ground states in the whole Hilbert space for a fixed total number of particles. In a population-imbalance-conserved subspace phase separation occurs at any energy splitting  $I$ . The main results are summarized in Fig.1. Unlike in usual superconductors where a state prepared at an arbitrary  $P_{im}$  and  $I$  generally is driven toward an equilibrium state with  $P_{im} = P_{im}^{eq}(I)$ , a cold atom state can only settle with the lowest energy state in the Hilbert subspace of a given initial population imbalance  $P_{im}$ . Phases in the inset of Fig. 1 (a) and (b) are for those lowest energy states with a given population difference  $P_{im}$  and density  $\rho$  in a given field  $I$ . In Fig. 1 (a) and (b) we present the scattering length dependence of critical population imbalance  $P_{c1}, P_{c2}$ .

The model we employ to study this subject is the standard one-channel model which is suitable for the discussion of superfluids near broad Feshbach resonances. The homogeneous states under consideration are BCS states with excess quasi-particles accommodating unpaired atoms or the population imbalance, i. e.,

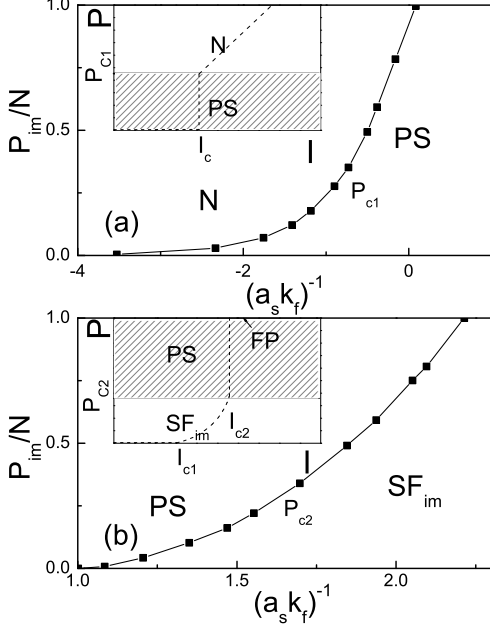


FIG. 1: The critical population imbalance as a function of scattering length. In (a)[(b)],  $P_{c1}(P_{c2})$  versus  $(a_s k_f)^{-1}$  for negative(positive) scattering length  $a_s$ .  $P_{c1}(P_{c2})$  is the critical value below(beyond) which phase separation takes place(see also inset). Here  $N$  stands for a normal state,  $PS$  for a phase separated state,  $SF_{im}$  for a superfluid with a finite *uniform* population imbalance, and  $FP$  for a fully polarized state. In (b), the phase separated state is constructed using a superfluid with a finite population difference and a fully polarized state. In inset, we show phases on the  $P_{im} - I$  plane. Shaded areas are for phase separated states; the dashed lines are the schematic equilibrium curves  $P_{im} = P_{im}^{eq}(I)$  for a given chemical potential, towards which the system is driven if an exchange of particles with a reservoir is allowed.

$\prod_{\mathbf{k} \in \Gamma} \gamma_{\mathbf{k}, \uparrow}^\dagger |BCS\rangle$  ( $\gamma_{\mathbf{k}, \uparrow}^\dagger$  is the creation operator of quasi-particles). These states are analogues of the breached-pair states discussed previously[7]. Notice here  $|BCS\rangle$  is a BCS state with a  $P_{im}$ -dependent gap  $\Delta(P_{im})$  and  $\gamma_{\mathbf{k}, \uparrow}^\dagger$  is the quasiparticle creation operator. The corresponding gap is self-consistently determined by the following gap equation in the presence of population imbalance

$$\frac{1}{\lambda_R} = \sum_{\mathbf{k}} \frac{1}{2E_{\mathbf{k}}} (1 - n_{\mathbf{k}, \uparrow}) - \sum_{\mathbf{k}} \frac{1}{2\varepsilon_{\mathbf{k}}} \quad (1)$$

with  $\varepsilon_{\mathbf{k}} = k^2/2m$ ,  $\xi_{\mathbf{k}} = \varepsilon_{\mathbf{k}} - \mu$ ,  $E_{\mathbf{k}} = \sqrt{\Delta^2 + \xi_{\mathbf{k}}^2}$  and  $n_{\mathbf{k}, \uparrow}$  is the occupation number of quasi particles at state  $\mathbf{k}$ , spin-up and  $\lambda_R$  is related to  $a_s$  by  $\lambda_R V = -4\pi a_s/m$ . Furthermore, only the lowest energy quasi-particle states are occupied so as to minimize the kinetic energy for

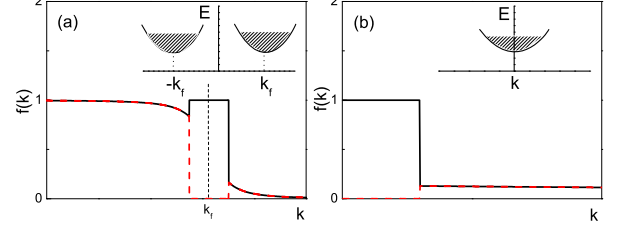


FIG. 2: The momentum distribution function  $f(k)$  of spin-up(solid line) and spin-down atoms(dashed line) in homogeneous states studied in this article. (a) For negative scattering length and positive chemical potential; (b) for positive scattering length and negative chemical potential. Inset: schematic of the occupation of quasi-particles.

given population imbalance.  $n_{\mathbf{k}, \uparrow}$  therefore takes the form of a step function

$$n_{\mathbf{k}, \uparrow} = \begin{cases} 1 & \text{if } |\varepsilon_{\mathbf{k}} - \mu| \leq \delta\xi \\ 0 & \text{if } |\varepsilon_{\mathbf{k}} - \mu| > \delta\xi \end{cases} \quad (2)$$

which is unity only when  $|\varepsilon_{\mathbf{k}} - \mu|$  is less than the cut-off energy  $\delta\xi$ . The energy of quasi-particles is  $E_{\mathbf{k}} - I$  and can be either positive or negative; the distribution function here is not the usual equilibrium one. The total number of these quasiparticles precisely yields the population imbalance as indicated in Fig. 2,

$$P_{im} = \sum_{\mathbf{k}} n_{\mathbf{k}, \uparrow} \quad (3)$$

Each state under consideration here is therefore the lowest energy homogeneous state in the corresponding constrained subspace. Finally, the total number of particles is given as

$$N = \sum_{\mathbf{k}} \left(1 - \frac{\xi_{\mathbf{k}}}{E_{\mathbf{k}}}\right) (1 - n_{\mathbf{k}, \uparrow}) + \sum_{\mathbf{k}} n_{\mathbf{k}, \uparrow} \quad (4)$$

The mean-field  $\mathcal{EP}$ ,  $\Omega = \langle \mathcal{H}_{BCS} \rangle - \mu N$  (or the free energy at  $T = 0$  but with  $P_{im}$  fixed) is

$$\Omega = \sum_{\mathbf{k}} (E_{\mathbf{k}} - I) n_{\mathbf{k}, \uparrow} + \sum_{\mathbf{k}} \left(\xi_{\mathbf{k}} - E_{\mathbf{k}} - \frac{\Delta^2}{2\varepsilon_{\mathbf{k}}}\right) + \frac{\Delta^2}{\lambda_R} \quad (5)$$

Taking into account Eq.(4) one can also easily obtain the energies of states with given  $N$  and  $P_{im}$ .

The  $\mathcal{EP}$  landscape of homogeneous states at different scattering length has been obtained. When the scattering length is negative and the magnitude is small, we find a set of homogeneous solutions  $\Delta(P_{im})$  to the gap equation for a given population imbalance  $P_{im}$ . The self-consistent BCS gap decreases as the magnetization  $P_{im}$

increases and becomes zero at a critical value as seen in Fig. 3 (b). The critical value of  $P_{im}$  is independent of the energy splitting as also indicated by vertical lines in Fig. 3 (a), (c) and (e). The cold atoms in this limit would have a continuous phase transition to a normal state if the spatial phase-separation were prohibited. The  $\mathcal{EP}$  of states with a given chemical potential and in the presence of a given energy splitting is plotted as a function of the population imbalance  $P_{im}$  in Fig. 3. Firstly, the BCS state represented by the solution at  $P_{im} = 0$  point becomes degenerate with a normal state (a solution with  $\Delta = 0$ ) at a critical magnetic field  $I_c = \Delta_0/\sqrt{2}$ . Secondly, a local minimum (a metastable normal state) and a maximum (the Sarma solution) appear when the energy splitting is between  $I = \Delta_0/2$  and  $I = \Delta_0$ ; here the normal and BCS state are interpolated by the Sarma solution as expected in the conventional BCS theory[4].

To find the ground state for a given conserved population imbalance, we examine the  $\mathcal{EP}$  landscape of the homogeneous states. We find that at *any given energy splitting* the energy curve is concave (down) when the population imbalance is small. For a given population difference, one constructs a mixed state which involves the BCS state and a normal state located at the end point of the concave part of the curve. These two states involved in the construction correspond to two degenerate states at the first order phase transition point and always have the same chemical potentials for each fermion species. For a given density  $\rho$  and  $P_{im}$ ,  $X$  the fraction of the BCS state and  $\mu$  should be determined self-consistently by the following conditions,

$$\begin{aligned} \rho &= \rho_{BCS}(\mu)X + \rho_N(\mu, \delta\mu = I_c(\mu))(1 - X), \\ P_{im} &= P_{im}(\mu, \delta\mu = I_c(\mu))(1 - X). \end{aligned} \quad (6)$$

Here  $\rho_{BCS(N)}$  is the density of a BCS (normal) state when the chemical potential difference between two species  $\delta\mu$  is equal to the critical energy splitting  $I_c$ ;  $P_{im}$  is the corresponding population imbalance of the normal state. The phase separation occurs when the population imbalance is smaller than a critical one. The critical value corresponds to the population imbalance at the end point of the concave-downwards part of the curve, or the solution to the above equation at  $X = 0$ . Above that critical value the homogeneous states regain stability. By carrying out similar analysis at different scattering length, we also obtain the scattering length dependence of the critical population imbalance (Fig. 1(a)).

When the scattering length becomes positive and especially when the chemical potential becomes negative, the  $\mathcal{EP}$  landscape experiences an important qualitative change. The part of curve for the small population imbalance becomes *convex* (or concave up) instead of concave (down). On the other hand, beyond a critical imbalance population the curve again is concave. A transition from

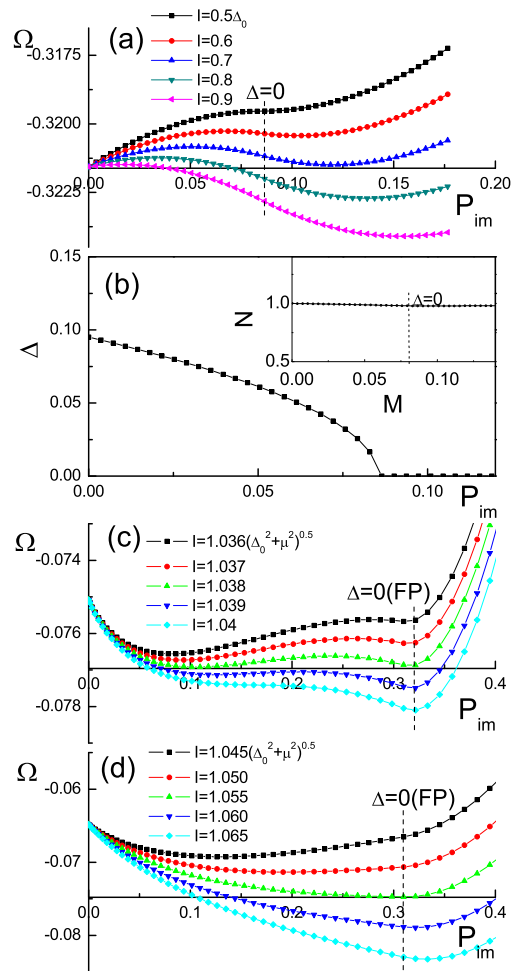


FIG. 3: In (a), (c) and (d) we show the energy potential as a function of the population imbalance  $P_{im}$  at different energy splitting  $I$  but with a fixed chemical potential. (a) is for a negative scattering length  $(a_s k_F^0)^{-1} = -1.40$  and  $\mu = 0.98\varepsilon_F^0$ ; (c) for positive scattering length near resonance  $(a_s k_F^0)^{-1} = 1.27$  and  $\mu = -1.68\varepsilon_F^0$ ; (d) for a small positive scattering length  $(a_s k_F^0)^{-1} = 1.56$  and  $\mu = -2.66\varepsilon_F^0$ .  $k_F^0$  is defined as the Fermi momentum for the density  $N_0/V$  at zero population imbalance  $P_{im} = 0$  and  $\varepsilon_F^0$  is the corresponding Fermi energy. In (b), we show the variation of  $\Delta$  and  $N$  as a function of  $P_{im}$  in the homogeneous solutions to Eq. (1)-(4) (with the same scattering length and chemical potential as in (a)). Notice in (c) and (d), all the states to the right of the vertical dashed line correspond to fully polarized states. Here  $N$  and  $P_{im}$  are expressed in unit of  $N_0$  and  $\Omega$  is in unit of  $0.75^{2/3}\varepsilon_F^0$ .

*convex to concave* as the population imbalance increases is a general feature of the landscape when the chemical potential is negative and again is independent of the energy splitting.

As the energy splitting increases, the global minimum along the curve shifts *continuously* from  $P_{im} = 0$  point into a uniform superfluid with a finite population imbalance

ance. This signifies a continuous transition from a BCS state to a uniform superfluid with population imbalance when the chemical potential becomes negative. Further increasing the energy splitting leads to an additional local minimum and local maximum (see Fig. 3 (c)). The new local minima located by the vertical dashed line represent *fully polarized states* and therefore the pairing amplitude associated with these states is zero, i.e.  $\Delta = 0$ . At an upper critical value, we obtain two degenerate solutions located at two ends of the concave part of the curve, one being a homogeneous superfluid with population imbalance and the other a fully polarized state. One uses these two states to construct a phase separated state since again the chemical potential for each fermion species can be shown to be the same. Phase separation occurs when the population imbalance exceeds a critical value specified by the left end of the concave curve in Fig.3(c) (i.e. the superfluid with uniform population imbalance). Note that in this case the density variation along a given curve is substantial. At a smaller positive scattering length or deep into the BEC side of the resonance, we find the concave-down section of a curve moves toward higher population imbalance and finally disappears in the  $\mathcal{EP}$  landscape (shown in Fig. 3 (d)). Homogeneous superfluids with population imbalance are always stable in this limit.

Before concluding we would like to make two comments. The first one is about the role of population imbalance relaxation (PIR). In the presence of PIR, the population imbalance takes a unique equilibrium value  $P_{im}^{eq}(I)$ ; phase separation of cold atoms in this limit (with the total number density fixed) needs a fine tuning in the energy splitting  $I$ . If the difference between the density of a BCS state and that of a normal state at the same chemical potential is negligible, the phase separation only occurs when  $I$  takes a critical value. Indeed, as illustrated before[12] the phase separation takes place in the vicinity of a critical splitting and the interval becomes to be exponentially small in the weakly interacting limit. In the view of this, the phase separation observed in Ref.[1, 2] in the *extreme quantum limit* (i.e. extremely slow imbalance relaxation) is distinct from phase separation phenomena in the opposite limit where only equilibrium states are considered. Meanwhile, in general the time-dependence of population imbalance can be expressed as  $P_{im}(t) = P_{im}(0) \exp(-t/\tau) + P_{im}^{eq}(I)(1 - \exp(-t/\tau))$  (here  $\tau$  is the imbalance relaxation time.). The temporal behavior of phase separation therefore does depend on the energy splitting  $I$ , though practically such dependence is always suppressed if the measurement time is much shorter than the relaxation time  $\tau$ .

The second remark is on the effect of confinement or finite size. In the presence of smooth potentials, the spatial variation of particle density effectively provides an ensemble of cold atoms superfluids at different chemical potentials. The phase separation occurs in a region

where the self-consistent chemical potential difference  $\delta\mu$  (determined by the population imbalance) is equal to the critical value  $\delta\mu_c$  for the local self-consistent chemical potential  $\mu(\mathbf{r})$ . However, if the confinement potential is hard-wall like, then the chemical potential difference could be *self-consistently* pinned in the vicinity of the critical value  $\delta\mu_c$  for the bulk density.

In conclusion, we have mapped out the  $\mathcal{EP}$  landscape for fermion states with population imbalance. This result might be the blueprint for the future studies of the dynamics of various competing states near Feshbach resonances. For instance it can be used to understand the energy released, during the phase separation, from a homogeneous state initially prepared and the evolution of initial states. The phase separation of fermion pairing states in a population imbalance conserved subspace turns out to be robust and needs no fine tuning in the energy splitting. This is also the limit where experiments were carried out and we believe the results obtained here will help to identify new interesting experimental opportunities in the future. We would like to thank Mike Forbes, Randy Hulet, Wolfgang Ketterle, Tony Leggett, and Boris Spivak for numerous discussions. This work is supported by a grant from the office of the Dean of Science at University of British Columbia and a Discovery grant from NSERC, Canada. FZ is an A. P. Sloan fellow.

- 
- [1] M. W. Zwierlein, et al., Science **311**, 492 (2006).
  - [2] G. B. Partridge, et al., Science **311**, 503 (2006).
  - [3] M. Clogston, Phys. Rev. Lett. **9**, 266 (1962).
  - [4] G. Sarma, J. Phys. Chem. Solids **24**, 1029 (1963).
  - [5] P. Fulde and R. A. Ferrell, Phys. Rev. **135**, A550 (1964).
  - [6] A. J. Larkin and Y. N. Ovchinnikov, Sov. Phys. JETP **20**, 762 (1965).
  - [7] W. V. Liu and F. Wilczek, Phys. Rev. Lett. **90**, 047002 (2003); M. Forbes et al., Phys. Rev. Lett. **94**, 017001 (2005); T. L. Ho and H. Zhai, cond-mat/0602568.
  - [8] P. F. Bedaque, H. Caldas and G. Rupak, Phys. Rev. Lett. **91**, 247002 (2003).
  - [9] M. Greiner, et al., Nature **426**, 537 (2003); C. A. Regal, et al., Phys. Rev. Lett. **92**, 040403 (2004); S. Jochim, et al., Science **302**, 2101 (2003); M. W. Zwierlein, et al., Phys. Rev. Lett. **91**, 250401 (2003); K. E. Strecker, et al., Phys. Rev. Lett. **91**, 080406 (2003).
  - [10] J. Carlson and S. Reddy, Phys. Rev. Lett. **95**, 060401 (2005).
  - [11] C. H. Pao, et al., cond-mat/0506437; D. T. Son and M. A. Stephanov, cond-mat/0507586.
  - [12] D. E. Sheehy and L. Radzihovsky, Phys. Rev. Lett. **96**, 060401 (2006).
  - [13] P. Pieri and G. C. Strinati, cond-mat/0512354; W. Yi and L. M. Duan, cond-mat/0601006; F. Chevy, cond-mat/0601122; T. N. De Silva and E. J. Mueller, cond-mat/0601314; M. Haque and H. T. C. Stoof, cond-mat/0601321.